Supporting information

Er^{3+} Self-sensitized Nanoprobe with Enhanced 1525 nm Downshifting Emission for NIR-IIb *in vivo* Bio-imaging

Wang Wang [a,b,e,†], Zhe Feng [c,†], Bai Li [d], Yulei Chang [a], Xu Li [b], Xu Yan [b], Runze Chen [c], Xiaoming Yu [f], Huiying Zhao [d], Geyu Lu [b], Xianggui Kong [a], Jun Qian [c,*] and Xiaomin Liu [a,b,*]

[a] State Key Laboratory of Luminescence and Applications, Changchun Institute of Optics, FineMechanics and Physics, Chinese Academy of Science, Changchun 130033, China E-mail: xgkong14@cimp.ac.cn (X.K.).

[b] State Key Laboratory of Integrated Optoelectronics, College of Electronic Science and Engineering, Jilin University, Changchun 130012, China E-mail: xiaominliu@jlu.edu.cn (X.L.).

[c] State Key Laboratory of Modern Optical Instrumentations, Centre for Optical and Electromagnetic Research, College of Optical Science and Engineering, Zhejiang University, HangZhou 310058, China E-mail: qianjun@zju.edu.cn (J.Q.).

[d] The First Hospital, Jilin University, Changchun 130021, China a. E-mail: hui_ying@jlu.edu.cn (H.Z.)

[e] University of the Chinese Academy of Sciences, Beijing 100049, China E-mail: 404669930@qq.com (W.W.)

[f] Women's Hospital, Zhejiang University School of Medicine, Hangzhou 310006, China E-mail: yuxiaoming@zju.edu.cn (X.Y.)

W. Wang and Z. Feng contributed equally to this work

Contents

1. Experimental

1.1. Reagents

$RECl_3 \cdot 6H_2O$ (RE: Er, Tm, Yb, Y, > 99%), oleic acid (OA, 90%), 1-octadecene (ODE, 90%), oleylamine (OM, 70%), CF_3COONa, were purchased from Sigma-Aldrich. RE_2O_3 (RE: Y, Lu, Gd, Nd) and Trifluoroacetic acid (CF_3COOH, >99.5%) was purchased from Aladdin. NaOH, NH_4F, methanol, acetone, ethanol and cyclohexane were purchased from GFS Chemical. All the chemicals were of analytical grade and there was no further purification unless otherwise noted.

1.2. Preparation of Nanoparticles

We employed a method named Ostwald ripening for synthesizing the β-$NaErF_4$: (0.0 mol%, 0.5 mol%, 1.0 mol%, 2.0 mol%, 3.0 mol%, 5.0 mol% and 15.0 mol%, respectively) Tm @$NaReF_4$ (Re: Y, Lu, Gd) and $NaYF_4$: 20%Yb, 2%Er @$NaYF_4$: 20%Nd core-shell nanoparticles.[1] The precursors of different kinds of shell should be prepared beforehand. And the synthesis of relative bare cores adopted from a previously reported procedure with some modifications.[2]

1.3. Synthesis of Bare Core β-$NaErF_4$: Tm Nanoparticles

In a typical procedure, 1.0 mmol $ErCl_3 \cdot 6H_2O$ and $TmCl_3 \cdot 6H_2O$ calculated by stoichiometric ratio were added into a three-neck flask (50 mL) together with 15.0 mL ODE and 6.0 mL OA. Then, a stir operation at 160 °C about 30 mins is conduct to the mixture under an atmosphere of argon. Afterwards, the mixture had been cooled down to room temperature after the solution was totally clear. Furthermore, a 4.0 mL methanol solution mixed with 2.5 mmol NaOH and 4.0mmol NH_4F was dropwise added into the mixture. An obvious opacity had been seen, then the system was heated to 70 °C and kept it 25 mins for removing the methanol solvent. Thereafter, a heating progress to 300 °C was conduct under the protection of argon. The temperature had been kept for 1.5 h after it came to 300 °C. Moreover, the product was washed firstly by acetone once and secondly by ethanol twice when it came to room temperature again. In the end, 8 mL cyclohexane was used for dispersing the nanoparticles.

1.4. $NaREF_4$ (RE: Y, Lu, Gd and Y doped with 20%Nd) Precursor

Firstly, 5 mmol RE_2O_3 (RE: Y, Lu, Gd and Nd) was mixed with 20 mL di-water and 20 mL CF_3COOH in a reactor and refluxed at 90 °C for 24 h. Then the solution was evaporated at 60 °C to get the $(CF_3COO)_3RE$ (RE: Y, Lu, Gd and Nd) without any

CF_3COOH and water for the following experiment. Then, 2.0 mmol CF_3COONa and 2.0 mmol $(CF_3COO)_3$ RE (RE: Y, Lu, Gd and Y doped with 20%Nd) were added into a 50 mL flask along with 6.0 mL OA, 10.0 mL ODE and 6.0 mL OM. A fiercely stirring at 160 °C about 30 mins is conduct to the mixture for dissolving the reagents. Afterwards, the system was heated to 290 °C for 1.0 h. The solution was cooled down to room temperature until it reacted with enough time. In the end, a centrifugation by ethanol was done to the final mixture and the product was dispersed in 8.0 mL ODE for subsequent use.

1.5. Synthesis of β-$NaErF_4$: 1.0% Tm @$NaREF_4$ (RE: Y, Lu, Gd)

Here, 2.0 ml cyclohexane solution containing 0.25 mmol the as-prepared β-$NaErF_4$: 1.0% Tm bare core nanoparticles were injected into a 50ml three-neck flask with 15.0 mL ODE and 6.0 mL OA. Then the system was heated to 90 °C and kept it 15 mins for removing the cyclohexane solvent. Afterwards, the mixture was heated to 300 °C. 2.0 mmol $NaREF_4$ (RE: Y, Lu, Gd) Precursor was injected into the reactor in twice with an interval reaction time of 45 mins. Once the reaction completed, the system was cooled down and centrifuged by acetone once and ethanol twice.

1.6. Synthesis of β-$NaErF_4$:Tm @$NaLuF_4$ with different Tm^{3+} ions doping concentration

In this section, we employed the same methods of core-shell construction as before. On this occasion, 2.0 mL of β-$NaErF_4$: (0.0 mol%, 0.5 mol%, 1.0 mol%, 2.0 mol%, 3.0 mol%, 5.0 mol% and 15.0 mol%, respectively) Tm solution with 0.25 mmol bare core NPs were added into the reactor along with 15.0 mL ODE and 6.0 mL OA. And the same removing procedure to cyclohexane solvent and heating procedure to the system as the previous one was conduct. Then 1.2 mmol $NaLuF_4$ Precursor was injected into the 50ml three-neck flask in twice with an interval reaction time of 45 mins. After reaction was finished, the solution was cooled down and the products were collected by a centrifugation procedure that firstly employed acetone once and secondly employed ethanol twice. Finally, the collections were dispersed in 4 mL cyclohexane.

1.7. Synthesis of β-$NaErF_4$:0.5%Tm @$NaLuF_4$ with different shell thicknesses

In this part, a strategy that *via* changing the amount of substance of $NaLuF_4$ Precursor was used for tuning the shell thicknesses coating to β-$NaErF_4$: 0.5% Tm bare core. By employing the same procedure as before, we just adjusted the amount of substance of $NaLuF_4$ Precursor from 0.10 mmol, 0.20 mmol, 0.35 mmol, 0.50

mmol, 0.70 mmol, 0.90 mmol, 1.20 mmol, 1.50 mmol and 1.80 mmol for preparing the target products in each reaction.

1.8. Synthesis of $NaYF_4$: 20%Yb, 2%Er @$NaYF_4$:20%Nd

In a typical procedure, 1.0 mmol $YCl_3 \cdot 6H_2O$, $YbCl_3 \cdot 6H_2O$ and $ErCl_3 \cdot 6H_2O$ calculated by stoichiometric ratio were added into a three-neck flask along with 15.0 mL ODE and 6.0 mL OA. Then, a stirring at 160 °C about 30 mins is conduct to the mixture. Next, the mixture had been cooled down to room temperature after the reactants were totally dissolved. Furthermore, a 4.0 mL methanol solution mixed with 2.5 mmol NaOH and 4.0 mmol NH_4F was dropwise added into the reactor. Then the system was heated to 70 °C and kept it for 25 mins to remove the methanol solvent. And then, the mixture was heating to 300 °C for 1.5 h. Moreover, the product was washed firstly by acetone once and secondly by ethanol twice when it came to room temperature again. As above, 8 mL cyclohexane was used for dispersing the nanoparticles. Finally, a coating progress by 0.90 mmol $NaREF_4$ (Y doped with 20%Nd) Precursor to 2.0 ml cyclohexane solution containing 0.25 mmol the as-prepared bare core was conduct to get the final product by Ostwald ripening.

1.9. PEGylation of β-$NaErF_4$: Tm @$NaLuF_4$ NPs

The synthesis of PEG-b-PCL was employed the methods in our previous work.[3] Typically, 4 mL (about 200 mg) of the core-shell nanoparticles dispersed in cyclohexane were injected into a 20 mL vial containing 800 mg PEG-b-PCL and 4mL of chloroform. Then, a 20 mins sonicate was proceeded to dissolve the polymer entirely. Afterwards, the solution was stirring at 80 °C 3 h to evaporate all of the organic solvent. The solution remained in the vial was collected by centrifugation and 4 mL of distilled water was used for redispersed the collection. Thereafter, a 220 nm PES membrane was employed to filter solution and get the final product. The PEG-b-PCL successful coated with the NPs confirmed by DLS measurement and the PEGylated nanoparticles remain stable in distilled water without variation of the hydrodynamic size, as shown in Figure S2 (Supporting Information).

1.10. Preparation of ligand-free $NaErF_4$:0.5%Tm @4.30nm $NaLuF_4$ NPs

In this part, we adopt a previous method to prepare the target product with some modifications.[4] Typically, 2 mL 0.1 M HCl solution was added to the 2 mL of $NaErF_4$:0.5%Tm @4.30nm $NaLuF_4$ cyclohexane solution. And then, a vigorous stirring procedure was employed to the mixture till the NPs had been transferred into the water phase. The NPs was collected by centrifugation with 12000 rpm for 15 mins. At

the end, the solid collection was washed by di-water for two times and dispersed in HCl aqueous solution (pH ≈ 2) for the subsequent test.

1.11. Animal preparation

All experiments involving experimental animals were approved by the Institutional Ethical Committee of Animal Experimentation of Zhejiang University and they were performed strictly compliant with "The National Regulation of China for Care and Use of Laboratory Animals". Institute of Cancer Research (ICR) mice (5-6 weeks old, female) were supplied from Zhejiang Academy of Medical Sciences (Hangzhou, China) and BALB/c nude mice (~5 weeks old, male) were provided from the SLAC laboratory Animal Co. Ltd. (Shanghai, China) and housed in the Laboratory Animal Center of Zhejiang University (Hangzhou, China).

1.12. Optical system of NIR-IIb fluorescence macroscopic imaging and in vivo NIR-IIb fluorescence whole-body imaging

As shown in Figure S3, the 800 nm laser beam emitted by the semiconductor laser (Suzhou Rugkuta Optoelectronics Co., Ltd., China) was collimated and expanded through the lens so that the sample can be uniformly illuminated. The emitting fluorescent signal was collected onto the InGaAs camera (Tekwin, China) through a prime lens (focal length: 50 mm, Edmund Optics). A 1500 nm long-pass filter (Thorlabs) was placed in front of the detector to extract the pure NIR-IIb signals. After anesthesia, the mice were placed on the imaging platform. The PEGylated β-$NaErF_4$:0.5% Tm @4.30nm $NaLuF_4$ nanoparticles (200 μL, 5 mg/mL) was injected into the tail vein, then the laser was turned on immediately and the image was recorded at different time points.

1.13. Optical system for NIR-IIb fluorescence microscopic imaging and in vivo NIR-IIb fluorescence cerebrovascular imaging

As shown in Figure S4, with the upright fluorescence microscope (RX50, Sunny, China), the 800 nm laser beam was expanded and introduced into the epi-illumination module. After reflected by the long-pass dichroic mirror (900 nm DMLP, Thorlabs), the excitation beam then uniformly irradiated the sample through the objective lens (LSM03, WD = 25.1 mm, Thorlabs). The NIR-IIb signals emitting from the sample were collected by the objective lens and then detected by the InGaAs camera through the tube lens after passing through the 1500 nm long-pass filter (Thorlabs). The mice were divided into two groups. The skulls of one group of mice were opened under the microscope after they were anesthetized, then round thin coverslips were mounted on the brain. The skulls of the other group of mice were

kept moist after their scalps were removed. After the heads of the two groups of mice were immobilized, the PEGylated β-$NaErF_4$:0.5% Tm @4.30nm $NaLuF_4$ nanoparticles were injected into their tail veins, the laser was turned on and the images were recorded.

1.14. *In vivo* NIR-IIb gastrointestinal tract imaging

The β-$NaErF_4$:0.5% Tm @4.30nm $NaLuF_4$ nanoparticles (200 μL, 5 mg/mL) were perfused into the stomach of nude mice. The images of the mice were recorded using the above-mentioned NIR-IIb fluorescence macroscopic imaging system.

1.15. NIR-IIb fluorescence bile duct imaging in the rat

After anesthetization, the rat was fixed on a platform with its abdomen open. Normal extrahepatic bile duct was observed and recorded immediately by NIR-IIb fluorescence macroscopy by retrograded injection of the PEGylated β-$NaErF_4$:0.5%Tm @4.30nm $NaLuF_4$ NPs (~20 μL, 5 mg/mL) through the puncture at lower end of the bile duct.

1.16. NIR-IIb fluorescence bladder imaging in the mouse

To achieve retrograde cystography, the PEGylated β-$NaErF_4$:0.5%Tm @4.30nm $NaLuF_4$ NPs (~20 μL， 5 mg/mL) was retrogradely injected into the bladder in the mouse with a 26G indwelling needle (Shanghai Kindly Enterprise Development Group Co., Ltd). The administered mice were then imaged under the NIR-IIb fluorescence macroscopic imaging system.

1.17 Characterization and quantum yield measurement

The transmission electron microscopy (TEM) measurements were carried out on a JEM 2100F TEM (200 kV). The scanning electron microscope (SEM) was measured on a Hitachi S-4800 field emission scanning electron microscope. The power diffraction (XRD) data were recorded on a Bruker D8-advance X-ray powder diffractometer with Cu target (λ = 1.5406 Å). The luminescence emission spectra were measured by Edinburgh-FLS 980 spectrophotometer with excitation sources of 980 and 800 nm laser diodes. And the fluorescence lifetimes were measured by Hamamatsu R9110 PMT single photon counting system as a detector. The absorption spectra were recorded by the Ocean Optics, Maya-2000 fluorescent fiber optic spectrometer. The dynamic light scattering (DLS) were gained by the Malern Zetasizer Nano ZSP nanophox. The absolute quantum yield (QY) measurement was test by using FL920

Spectrometer (EDINBURGH) along with a calibrated integrating sphere under 800 nm CW diode laser at 0.81 W/cm^2 with 5 times scanning.

2. Supporting Figures, Tables and Video.

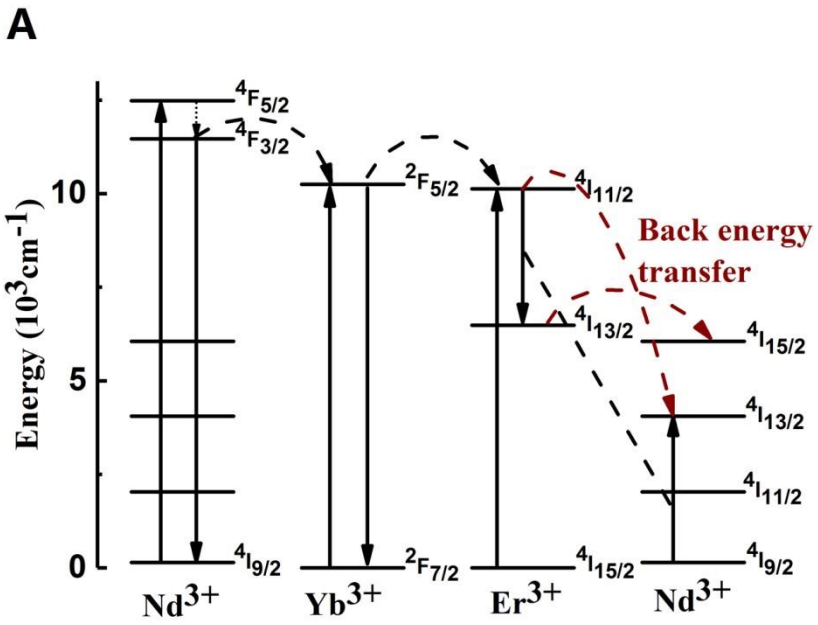

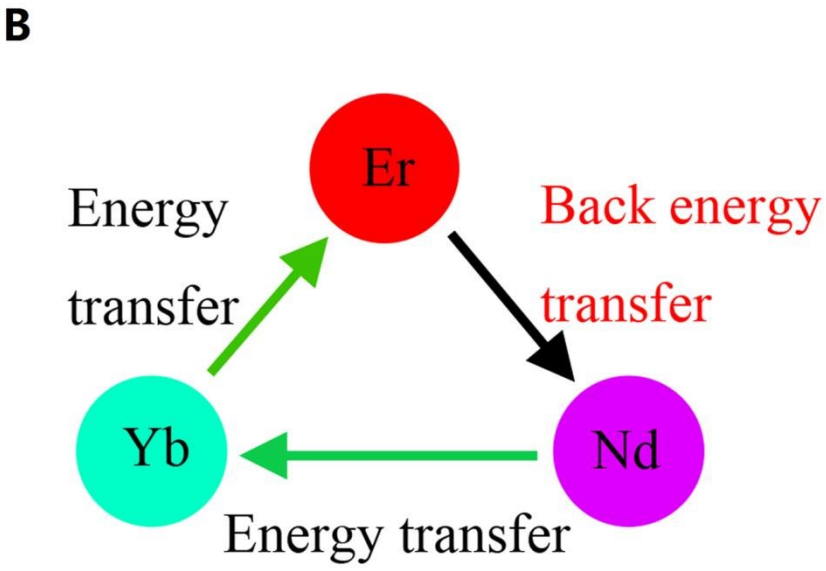

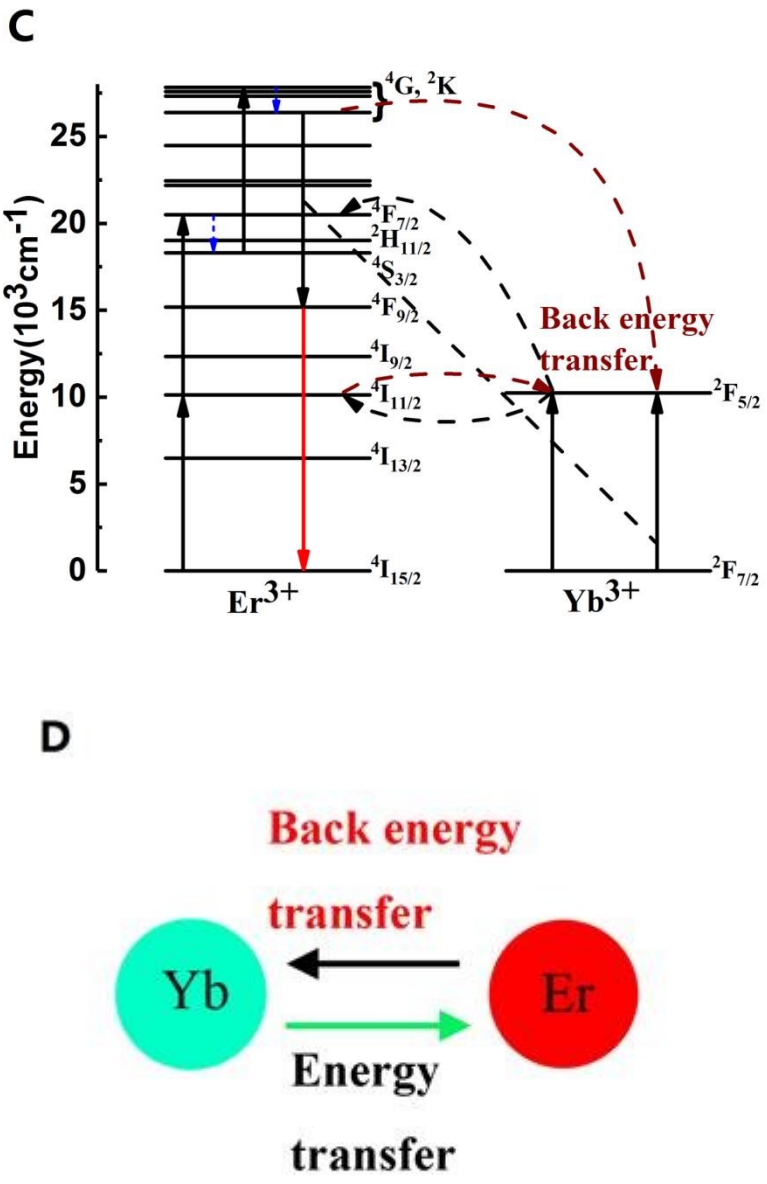

Figure S1. (A-B) Energy-level diagrams and Schematic illustration depicting the energy transfer between Nd^{3+}, Yb^{3+}, and Er^{3+} ions under 800 nm excitation. Here, the BET (back energy transfer) progress can be described as two conditions after the energy transfer to Er^{3+} ions from the excited Nd^{3+} ions. One is that the energy populated at $^4I_{11/2}$ energy level of Er^{3+} ions via a cross relaxation progress populating the $^4I_{13/2}$ energy level of Nd^{3+} ions. The other is that the energy populated at $^4I_{13/2}$ energy level of Er^{3+} ions directly transfer to the $^4I_{15/2}$ energy level of Nd^{3+} ions. (C-D) Energy-level diagrams and Schematic illustration depicting the energy transfer between $Yb^{3+}$and Er^{3+} ions under 980 nm excitation. Just like A & B, the BET progress

in Yb-Er system could also be summarized into two cases. The first case is that the energy populated at ^4G and ^2K energy level of Er^{3+} ions via a cross relaxation progress populating the $^2F_{5/2}$ energy level of Yb^{3+} ions. The second one is that the energy populated at $^4I_{11/2}$ energy level of Er^{3+} ions directly transfer to the $^2F_{5/2}$ energy level of Yb^{3+} ions.

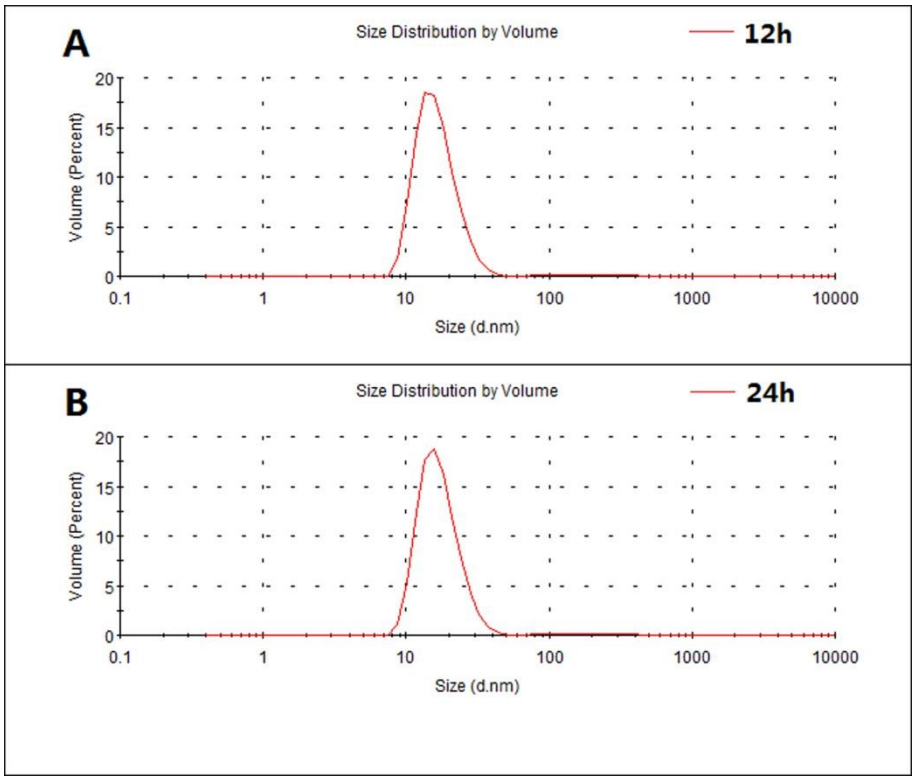

Figure S2. Dynamic light scattering (DLS) measurements of PEGylated $NaErF_4$:0.5% Tm @4.30nm $NaLuF_4$ core-shell NPs in distilled water at 12 and 24 h. And no aggregation was observed.

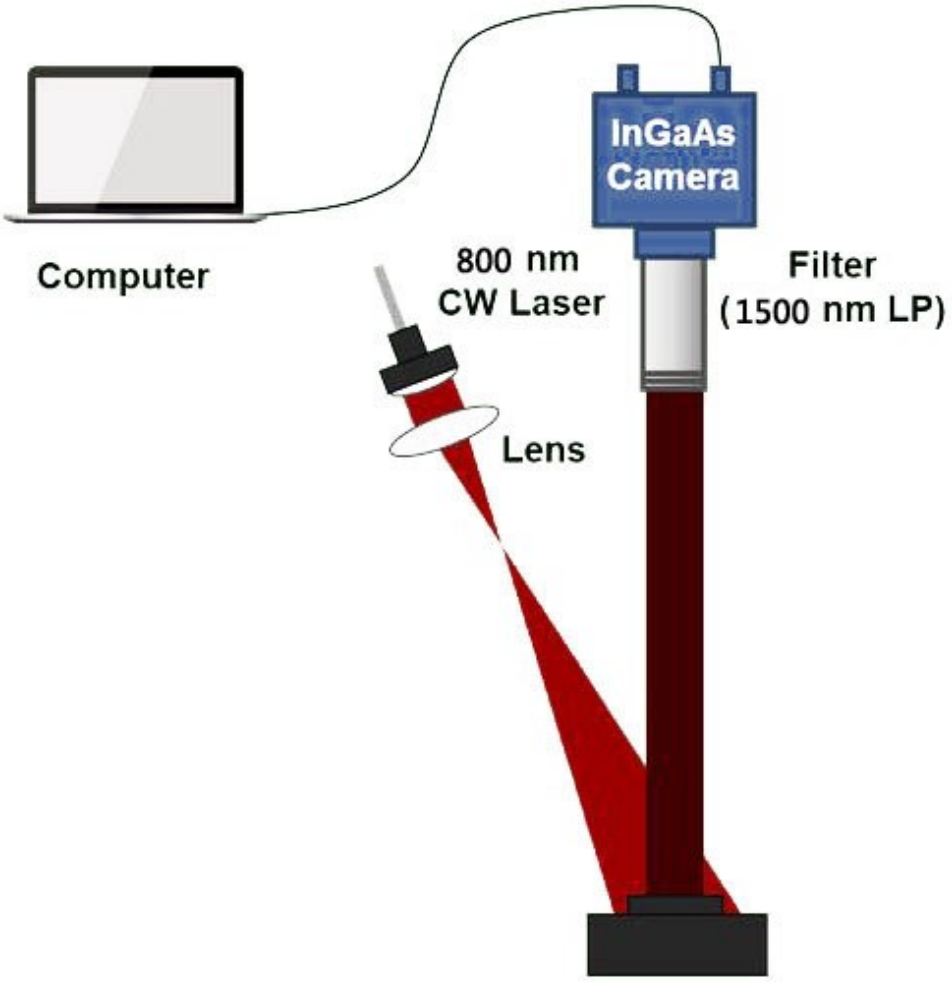

Figure S3. NIR-IIb fluorescence macroscopic imaging system.

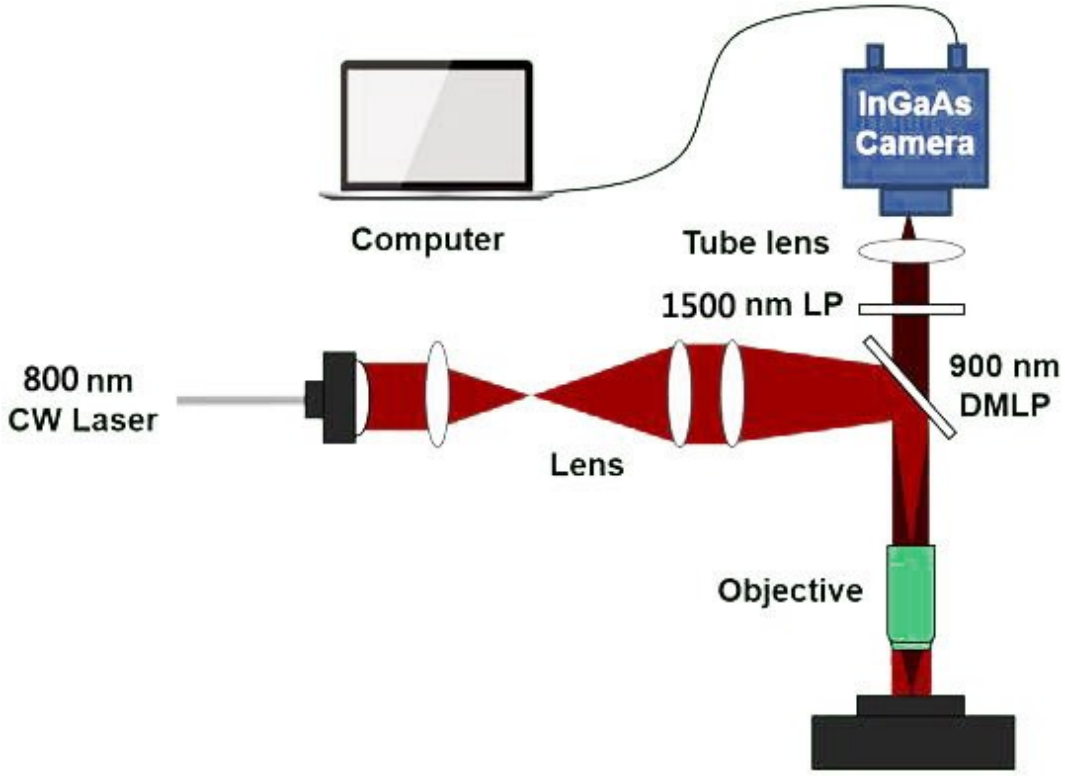

Figure S4. Schematic illustration of the NIR-IIb fluorescence microscopic imaging system.

A

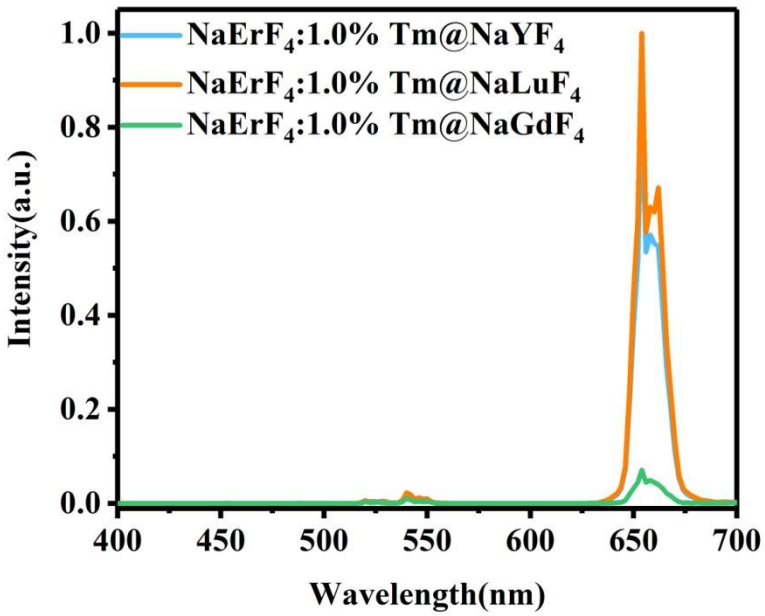
NaErF4:1.0% Tm@NaYF4
NaErF4:1.0% Tm@NaLuF4
NaErF4:1.0% Tm@NaGdF4
Intensity(a.u.)
Wavelength(nm)
1.0
0.8
0.6
0.4
0.2
0.0
400
450
500
550
600
650
700

B

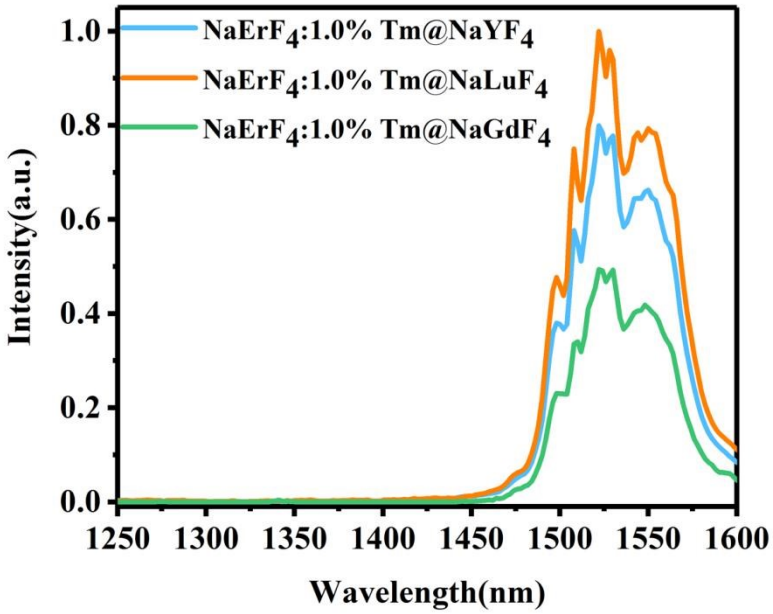
NaErF4:1.0% Tm@NaYF4
NaErF4:1.0% Tm@NaLuF4
NaErF4:1.0% Tm@NaGdF4
Intensity(a.u.)
Wavelength(nm)
1.0
0.8
0.6
0.4
0.2
0.0
1250
1300
1350
1400
1450
1500
1550
1600

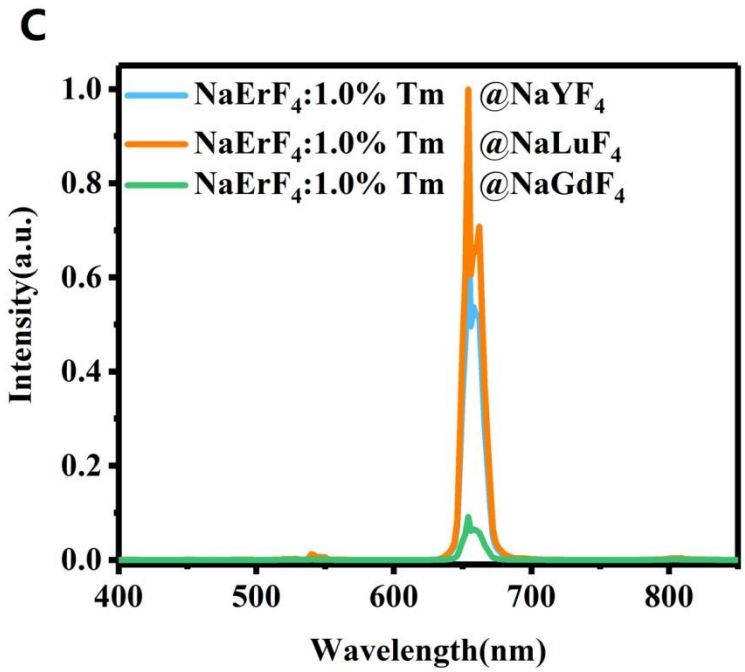

Figure S5. (A) Pictures show the upconversion emission spectra of cyclohexane solutions containing $NaErF_4$: 1.0%Tm @$NaYF_4$, $NaErF_4$: 1.0%Tm @$NaLuF_4$ and $NaErF_4$: 1.0%Tm @$NaGdF_4$ core-shell nanoparticles by 800 nm excitation (0.88 W/cm^2). (B-C) 1525 nm downshifting emission and upconversion emission spectra of cyclohexane solutions containing $NaErF_4$: 1.0%Tm @$NaYF_4$, $NaErF_4$: 1.0%Tm @$NaLuF_4$ and $NaErF_4$: 1.0%Tm @$NaGdF_4$ core-shell nanoparticles by 980 nm excited (2.49 W/cm^2), respectively.

Table S1. Summary of Structural Information for Core-Shell Nanoparticles

Smaple	Size (nm)	Lattice Constant a (Å)	Lattice Constant a mismatch	Lattice Constant c (Å)	Lattice Constant c mismatch
Core	**18.0±1.5**	**5.976**	**——**	**3.910**	**——**
$NaYF_4$ shelled	**31.7±2.0**	**6.016**	**+ 0.67%**	**3.932**	**+ 0.56%**
$NaLuF_4$ shelled	**31.7±2.0**	**5.964**	**- 0.20%**	**3.900**	**- 0.26%**
$NaGdF_4$ shelled	**31.1±2.1**	**6.032**	**+ 0.94%**	**3.948**	**+ 0.97%**

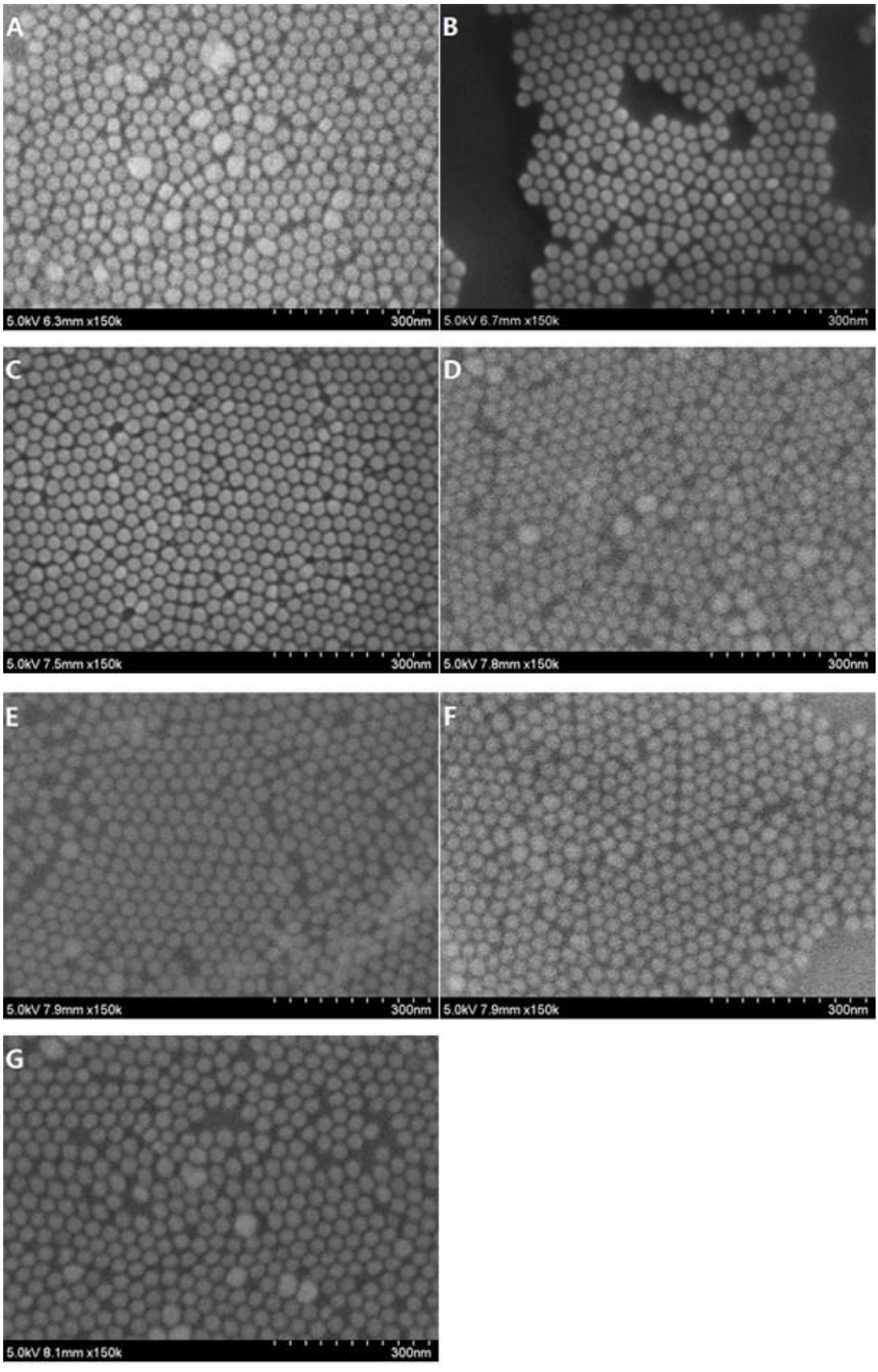
A
5.0kV 6.3mm x150k
300nm
B
5.0kV 6.7mm x150k
300nm
C
5.0kV 7.5mm x150k
300nm
D
5.0kV 7.8mm x150k
300nm
E
5.0kV 7.9mm x150k
300nm
F
5.0kV 7.9mm x150k
300nm
G
5.0kV 8.1mm x150k
300nm

Figure S6. Micrographs of core-shell nanoparticles. (A-G) These SEMs show the quasi-spherical morphology and mono-dispersity of the as-prepared $NaErF_4$: 0.0%Tm @$NaLuF_4$, $NaErF_4$: 0.5%Tm @$NaLuF_4$, $NaErF_4$: 1.0%Tm @$NaLuF_4$, $NaErF_4$: 2.0%Tm @$NaLuF_4$, $NaErF_4$: 3.0%Tm @$NaLuF_4$, $NaErF_4$: 5.0%Tm @$NaLuF_4$ and $NaErF_4$: 15%Tm @$NaLuF_4$ core-shell nanoparticles, respectively. The average sizes or diameters of these core-shell nanoparticles are about 29 nm and the scale bar is 300 nm.

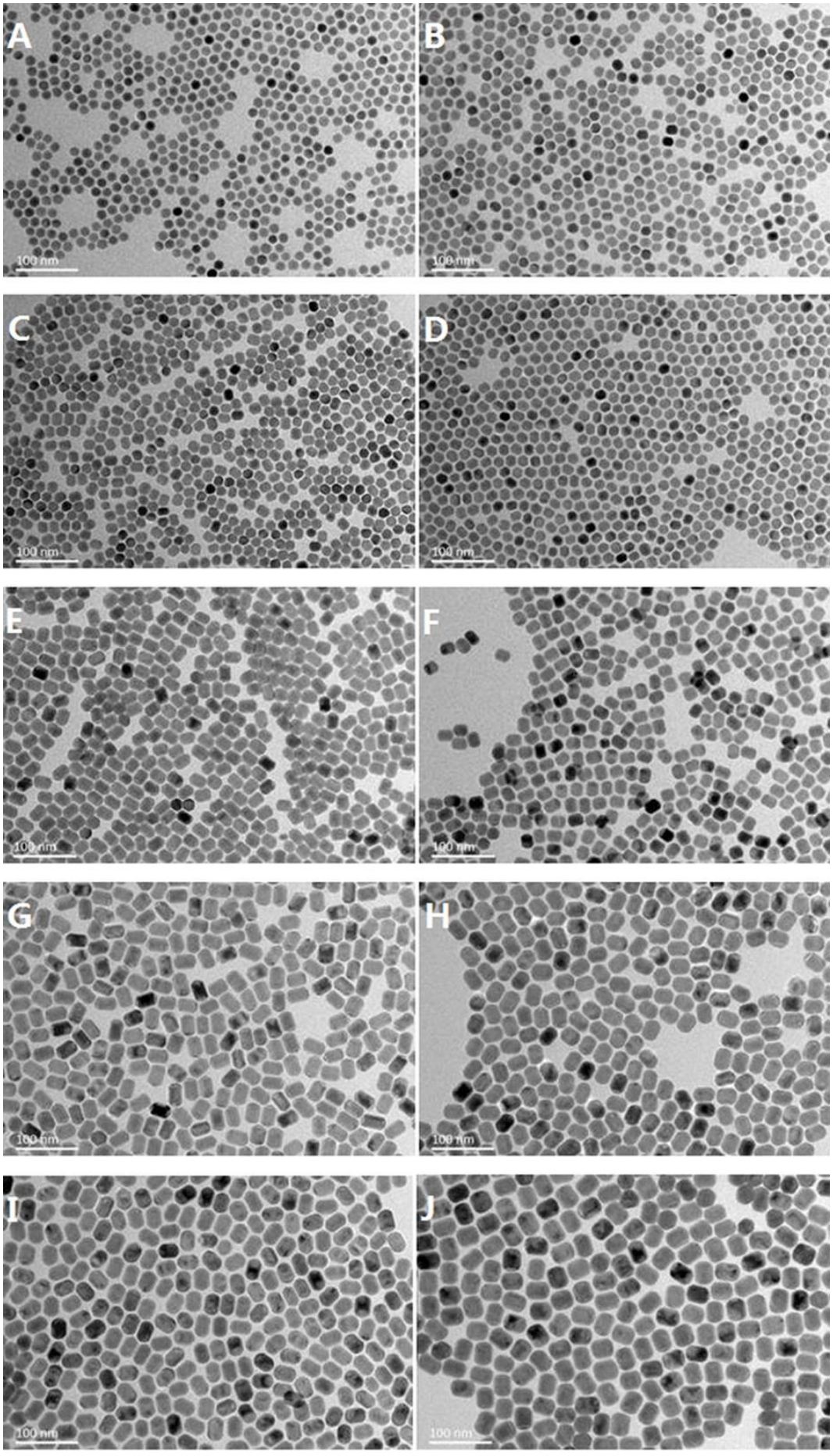
A
100 nm
B
100 nm
C
100 nm
D
100 nm
E
100 nm
F
100 nm
G
100 nm
H
100 nm
I
100 nm
J
100 nm

Figure S7. Micrographs of core-shell nanoparticles. (A-J) These TEMs are mainly showing the rod-like morphology and mono-dispersity of the as-prepared $NaErF_4$:0.5%Tm @0.00nm $NaLuF_4$, $NaErF_4$:0.5%Tm @0.71nm $NaLuF_4$, $NaErF_4$:0.5%Tm @1.21nm $NaLuF_4$, $NaErF_4$:0.5%Tm @1.55nm $NaLuF_4$, $NaErF_4$:0.5%Tm @2.40nm $NaLuF_4$, $NaErF_4$:0.5%Tm @2.25nm $NaLuF_4$, $NaErF_4$:0.5%Tm @4.30nm $NaLuF_4$, $NaErF_4$:0.5%Tm @5.31nm $NaLuF_4$, $NaErF_4$:0.5%Tm @4.97nm $NaLuF_4$ and $NaErF_4$:0.5%Tm @7.38nm $NaLuF_4$ core-shell nanoparticles, respectively. Their aspect ratios are in the range of 0.69 and 0.81. The scale bar is 100 nm. Because of the rod-like morphology of these core-shell nanoparticles, the thinner diameters are used as the standard of the shell thicknesses statistics for these core-shell nanoparticles.

Table S2.

In our design of the experiment, 10 different shell thicknesses from 0.0 nm to 9.0 nm were planned to prepare. For the rod-like morphology of these core-shell nanoparticles, the thinner diameters are used as the standard of the shell thicknesses statistics for these core-shell nanoparticles. The error of the shell thickness was calculated by Gaussian error propagation ($\sqrt{(\Delta core)^2 + (\Delta shell)^2}$) of the uncertainty in the size distribution from the TEM images of the core (Δcore) and core-shell nanocrystals (Δshell).

Desired shell thickness (nm)	Measured shell the thinner thickness (nm)	Average the thinner diameter (nm)	Aspect ratio
0.0	**0.00 ± 1.2**	**15.45 ± 1.2**	**1**
1.0	**0.71 ± 1.8**	**16.87 ± 1.3**	**1**
2.0	**1.21 ± 1.8**	**17.87 ± 1.4**	**0.79**
3.0	**1.55 ± 1.8**	**18.11 ± 1.4**	**0.80**
4.0	**2.40 ± 1.9**	**20.25 ± 1.5**	**0.78**
5.0	**2.25 ± 2.1**	**19.95 ± 1.7**	**0.79**
6.0	**4.30 ± 2.2**	**24.05 ± 1.8**	**0.69**
7.0	**5.31 ± 2.1**	**26.07 ± 1.7**	**0.78**
8.0	**4.97 ± 2.3**	**25.38 ± 2.0**	**0.70**
9.0	**7.38 ± 2.2**	**30.21 ± 1.9**	**0.81**

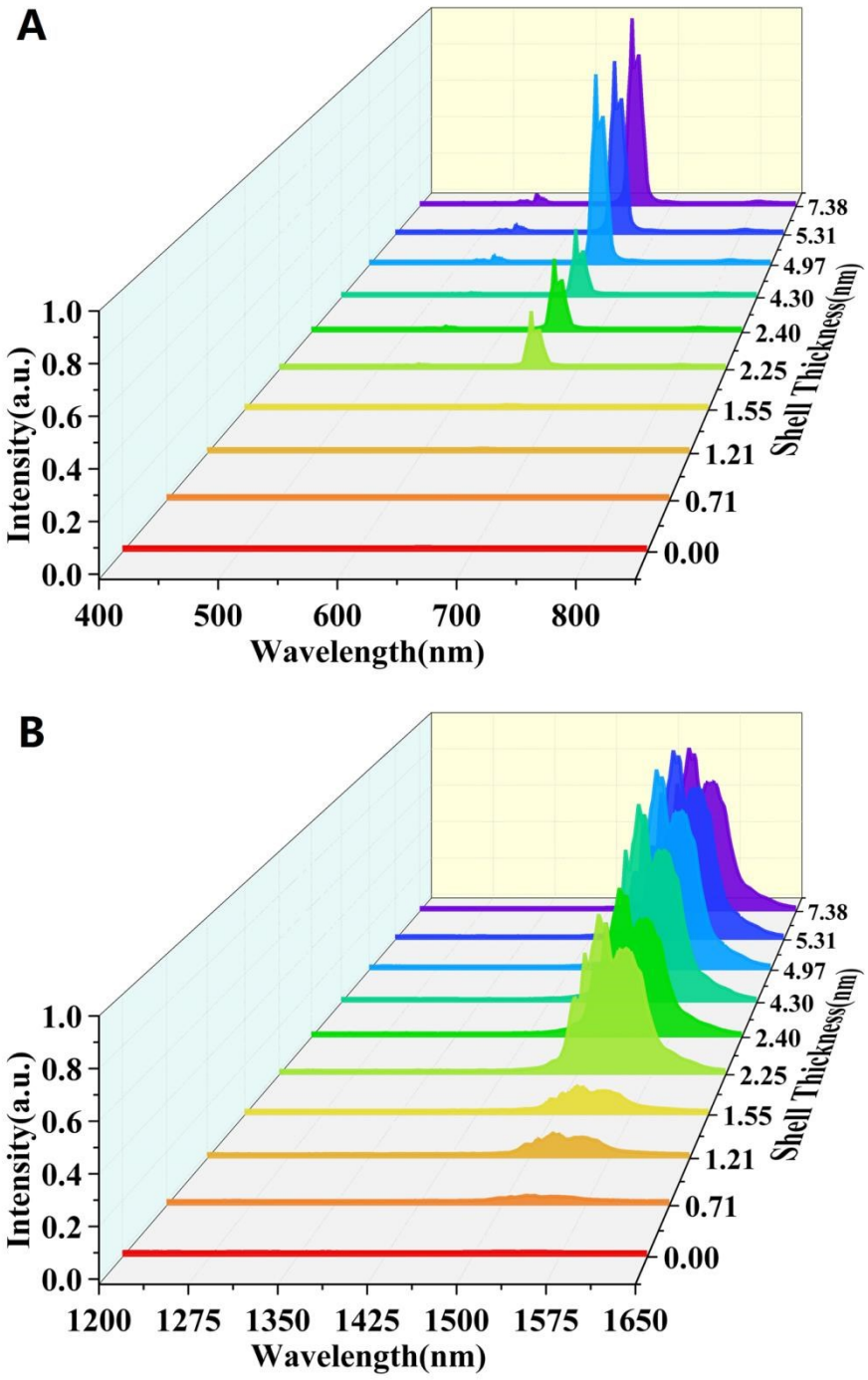
A
Intensity(a.u.)
1.0
0.8
0.6
0.4
0.2
0.0
400
500
600
700
800
Wavelength(nm)
7.38
5.31
4.97
4.30
2.40
2.25
1.55
1.21
0.71
0.00
Shell Thickness(nm)
B
Intensity(a.u.)
1.0
0.8
0.6
0.4
0.2
0.0
1200
1275
1350
1425
1500
1575
1650
Wavelength(nm)
7.38
5.31
4.97
4.30
2.40
2.25
1.55
1.21
0.71
0.00
Shell Thickness(nm)

C

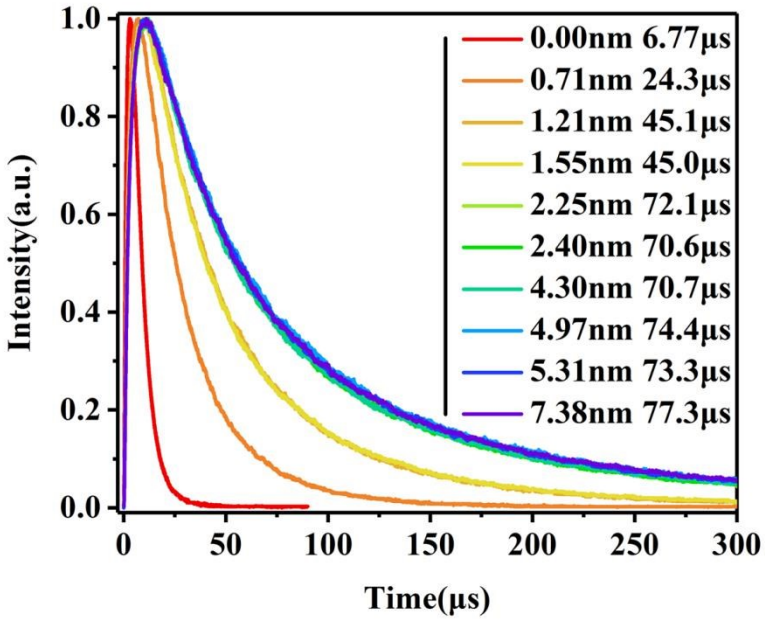
Intensity(a.u.)
Time(μs)
0.00nm 6.77μs
0.71nm 24.3μs
1.21nm 45.1μs
1.55nm 45.0μs
2.25nm 72.1μs
2.40nm 70.6μs
4.30nm 70.7μs
4.97nm 74.4μs
5.31nm 73.3μs
7.38nm 77.3μs

D

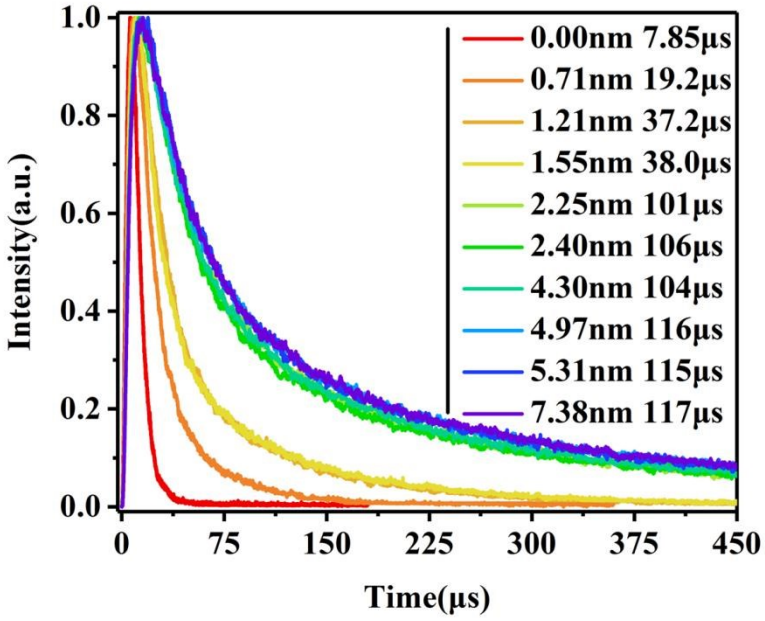
Intensity(a.u.)
Time(μs)
0.00nm 7.85μs
0.71nm 19.2μs
1.21nm 37.2μs
1.55nm 38.0μs
2.25nm 101μs
2.40nm 106μs
4.30nm 104μs
4.97nm 116μs
5.31nm 115μs
7.38nm 117μs

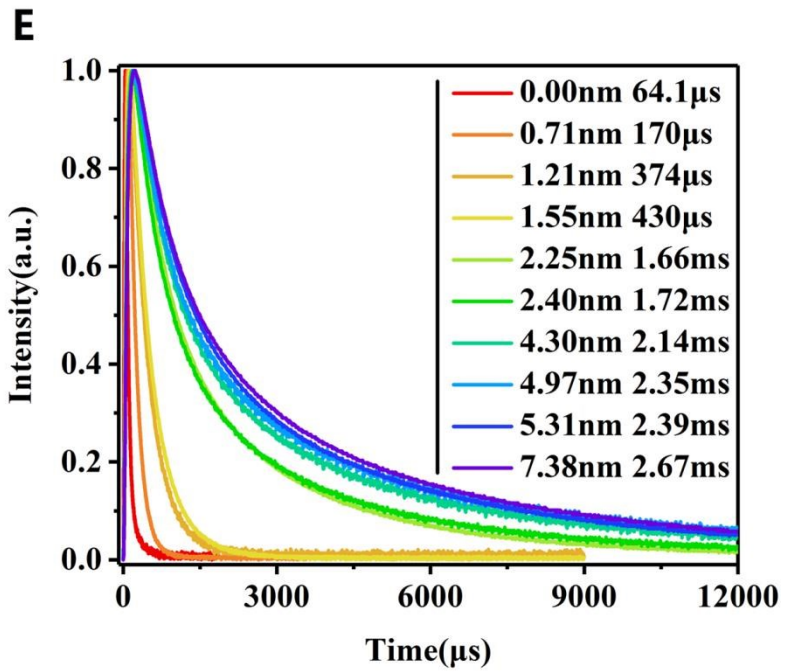

Figure S8. (A-B) These picture give the upconversion emission and 1525 nm Downshifting emission spectra of cyclohexane solutions containing the as-prepared $NaErF_4$:0.5%Tm@0.00nm $NaLuF_4$, $NaErF_4$:0.5%Tm@0.71nm $NaLuF_4$, $NaErF_4$:0.5%Tm@1.21nm $NaLuF_4$, $NaErF_4$:0.5%Tm@1.55nm $NaLuF_4$, $NaErF_4$:0.5%Tm@2.25nm $NaLuF_4$, $NaErF_4$:0.5%Tm@2.40nm $NaLuF_4$, $NaErF_4$:0.5%Tm@4.30nm $NaLuF_4$, $NaErF_4$:0.5%Tm@4.97nm $NaLuF_4$, $NaErF_4$:0.5%Tm@5.31nm $NaLuF_4$ and $NaErF_4$:0.5%Tm@ 7.38nm $NaLuF_4$ core-shell nanoparticles by 980 nm excited (7.31 W/cm^2)， respectively. (C-E) The three figure show the corresponding 540 nm (Er^{3+}:$^4S_{3/2}$→$^4I_{15/2}$), 650 nm (Er^{3+}:$^4F_{9/2}$→$^4I_{15/2}$) and 1525 nm (Er^{3+}:$^4I_{13/2}$→$^4I_{15/2}$) luminescence decay curve and their relevant lifetime values of these core-shell nanoparticles with different shell thicknesses under 980 nm excitation, respectively.

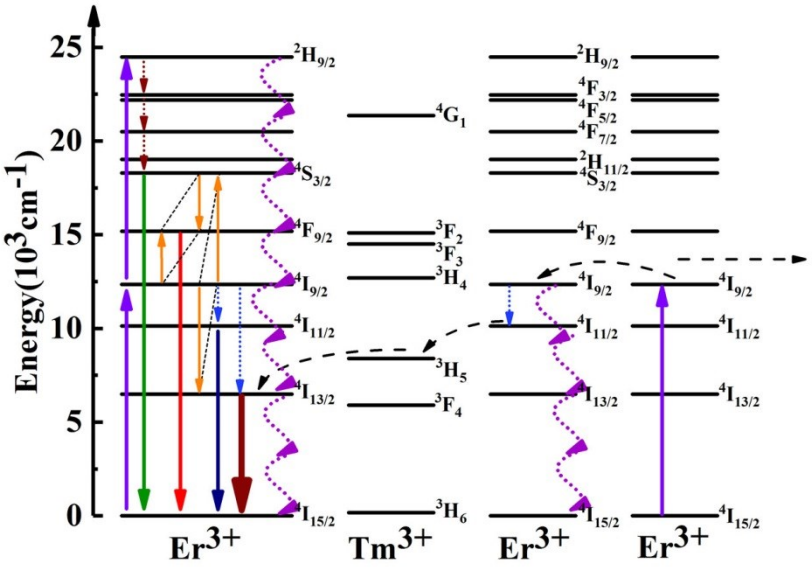

Figure S9. Energy level diagrams of Er^{3+} & Tm^{3+} ions and the proposed luminescence mechanisms with the surface quenching progress for $NaErF_4$:Tm core-only nanoparticles under excitation with a 800 nm diode laser.

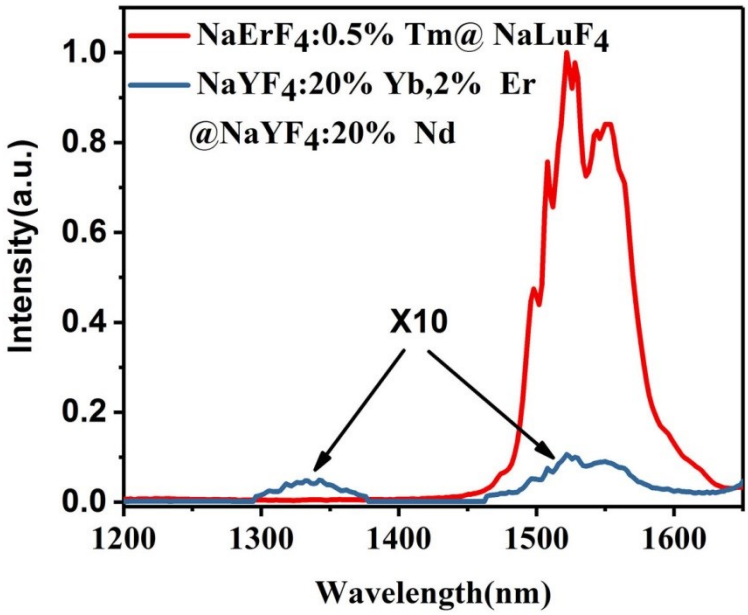

Figure S10. Downshifting emission spectra of cyclohexane solutions containing $NaErF_4$:0.5% Tm@4.30nm $NaLuF_4$ and $NaYF_4$:20%Yb, 2%Er@ 4.5nm $NaYF_4$:20%Nd core-shell nanoparticles by 800 nm excited (4.04 W/cm^2), respectively. And the absolute NIR-IIb luminescence quantum yields of $NaYF_4$: 20%Yb, 2%Er@ 4.5nm $NaYF_4$: 20%Nd is about 0.15% (800 nm CW diode laser: 0.81 W/cm^2).

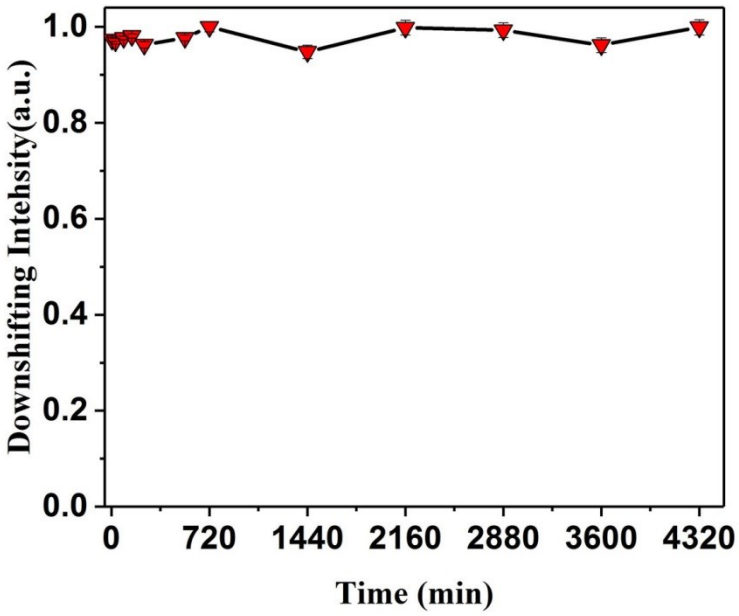

Figure S11. The picture shows the relationship of time-dependent downshifting emission intensity of ligand-free $NaErF_4$:0.5%Tm@4.30nm $NaLuF_4$ NPs by 800nm excited (2.41 W/cm^2), and the sampling time are determined by 5min, 0.5 h, 1.5 h, 2.5 h, 4 h, 9 h, 12 h, 24 h, 36 h, 48 h, 60 h, 72 h after NPs were dispersed in HCl aqueous solution (pH≈2), respectively.

Video S1. The video of gastrointestinal peristalsis. Exposure time: 50 ms.

References

1 H. Qian, Y. Zhang, Synthesis of Hexagonal-Phase Core-Shell $NaYF_4$ Nanocrystals with Tunable Upconversion Fluorescence, *Langmuir.* 2008, ***24***, 12123.

2 N. Johnson, A. Korinek, C. Dong, F. Veggel, Self-Focusing by Ostwald Ripening: A Strategy for Layer-by-Layer Epitaxial Growth on Upconverting Nanocrystals, *J. Am. Chem. Soc.* 2012, ***134***, 11068.

3 X. Liu, I. Que, X. Kong, Y. Zhang, L. Tu, Y. Chang, T. Wang, A. Chan, C. Löwikb, H. Zhang, *In vivo* 808 nm image-guided photodynamic therapy based on an upconversion theranostic nanoplatform, *Nanoscale*. 2015, ***7***, 14914.

4 J. Zuo, L. Tu, Q. Li, Y. Feng, I. Que, Y. Zhang, X. Liu, B. Xue, L. Cruz, Y. Chang, H. Zhang, X. Kong, Near Infrared Light Sensitive Ultraviolet−Blue Nanophotoswitch for Imaging-Guided “Off− On” Therapy,*ACS Nano.* 2018, ***12***, 3217.